JMEPEG (2008) 17:793–801
DOI: 10.1007/s11665-008-9237-1

1059-9495/$19.00

Corrosion Behavior of 316LN and 316 Stainless Steels During Long-term Exposure to Aerated 0.5 M NaCl Using Electrochemical Noise Technique

M.G. Pujar, N. Parvathavarthini, Sidhartha S. Jena, B.V.R. Tata, R.K. Dayal, and H.S. Khatak

(Submitted July 27, 2007; in revised form February 19, 2008)

In the present work 316LN as well as 316 stainless steel (SS) coupons each of dimensions (0.025 × 0.018 × 0.006 m^3) in well-polished condition were used as two nominal electrodes which were immersed in the aerated solution of 0.5 M NaCl. Correlated current and potential electrochemical noise (EN) signals were collected at 1 Hz sampling frequency for 1 h daily over a period of 30 days. The detrended EN data were used to calculate the noise resistance (R_N) as well as the spectral noise resistance at zero frequency (R^o_{SN}) values and other statistical parameters. To study the nature of pits and distribution of their diameters as well as depths, extensive observations of the pitted and the blank specimens were carried out using Confocal Laser Scanning Microscopy (CLSM). The current and the potential records of the two alloys showed distinct differences in their corrosion behavior. It was observed that within less than 4 h of immersion, 316SS showed signals indicative of unstable pitting and onset of stable pitting was noticed after 48 h of exposure. However, until about 24 h, 316LN showed just the random signals and unstable pitting was observed after 28 h. The signals clearly indicated continuous growth of the stable pits in 316SS as against the repassivation of the unstable pits in 316LN after 7 days exposure. It was observed that R_N values showed a continuous decrease in the case of 316SS, but were quite stable in the case of 316LN over the exposure period. Concurrent to these observations it was observed that 316SS specimen was extensively pitted. The frequency distributions of pit diameters as well pit depths were observed to be highest at 10-20 µm and 5-10 µm, respectively. However, pits with as large as 70-80 µm diameter and as deep as 20-25 µm too were observed. No pits were observed in case of 316LN even after 30 days of exposure, an observation that corroborates well with the stable R_N values. Thus, in the present investigation, the long-term tests using EN technique coupled with CLSM studies conclusively prove that many unstable pits initiated in 316SS turn into stable ones resulting in insidious localized corrosion attack whereas the unstable pits initiated in 316LN get passivated in the simulated coastal environment.

Keywords confocal microscopy, electrochemical noise, pitting corrosion, 316LN, 316SS

1. Introduction

Type 316L(N) austenitic stainless steel is the currently favored structural material in the primary side of Prototype Fast Breeder Reactor (PFBR). The choice of this material is based on its resistance to sensitization and adequate high-temperature mechanical properties. It is being used in many structural components such as main vessel, safety vessel, inner vessel, auxiliary grid plate, fuel transfer machines, intermediate heat exchangers, and core support structures because of its adequate strength, corrosion resistance, good weldability, and compatibility with liquid sodium. Low-carbon grades have been chosen to ensure freedom from sensitization during welding of the components and to avoid the risk of chloride stress corrosion cracking during storage in coastal site of Kalpakkam. Since low-carbon grades have lower strength than normal grades, nitrogen is specified as an alloying element to improve the mechanical properties so that the strength is comparable to 316SS.

However, several austenitic steels suffer extensive pitting or localized corrosion in the presence of halide ions (Ref 1). The nucleation sites of pits are usually found to be associated with nonmetallic inclusions (NMI) on SS. In particular, sulfide inclusions such as MnS and FeS were shown to be the potential sites in the extensive works of Wranglen (Ref 2), Eklund (Ref 3), and others (Ref 4-7). They have all clearly shown that the dissolution of a sulfide inclusion is the initial step in pit propagation at this site in Cl^- ion-bearing neutral and acidic solutions. Various alloying elements have been added to stainless steel, but only Cr, Mo, and N were found to be effective in promoting the resistance to localized corrosion (Ref 8). An index, known as pitting resistance equivalence number (PREN), has been widely used to predict the pitting corrosion resistance of stainless steels. It is expressed as PREN = %Cr + 3.3 (%Mo) + 16 (%N) (Ref 8). It indicates that increase in the concentration of Cr, Mo, and N in the steel will result in increased PREN and pitting potentials, but it is

M.G. Pujar, N. Parvathavarthini, R.K. Dayal, and **H.S. Khatak**, Corrosion Science and Technology Division (CSTD), Indira Gandhi Centre for Atomic Research (IGCAR), Kalpakkam 603 102, India; and **Sidhartha S. Jena** and **B.V.R. Tata**, Materials Science Division (MSD), IGCAR, Kalpakkam 603 102, India. Contact e-mail: pujar55@gmail.com.

expected that nitrogen would have much greater effect, since it has a factor of 16 in the equation. This is in comparison with 3.3 for molybdenum and 1 for chromium. The beneficial effects of nitrogen, as an alloying element, toward the mechanical and corrosion properties of many austenitic SS have been well recognized over the last two decades. In particular, it has been reported that nitrogen alloying can lead to improvements in pitting resistance of the alloys in Cl^- ion-bearing neutral and acidic solutions (Ref 9, 10). Several mechanisms have been proposed to explain the beneficial role of nitrogen in stainless steel. A plausible theory suggested that nitrogen in stainless steel will dissolve during corrosion process and consume the acid in pit by a reaction of $[N] + 4H^+ + 3e^- \rightarrow NH_4^+$. This causes a local neutralizing effect on the acidic environment inside the pits on the corrosion surface, leading to a decreased growth rate of a pit (Ref 11, 12). Other theories include: (1) enrichment of nitrogen on the passivated surface stabilizes the film, and prevents attack of anions like (Cl^-); (2) produced nitrate ions improve the resistance to pitting corrosion; (3) nitrogen addition stabilizes the austenitic phase (Ref 13, 14).

It is also well known that the accelerated DC corrosion tests like potentiodynamic anodic polarization studies conventionally used to determine the pitting potential (E_{pp}) of an alloy in a given medium can lead to the irreversible changes or damage to the specimen due to the dissolution during active polarization and hence are not preferred sometimes. Electrochemical noise (EN) technique has become quite popular in recent years most likely due to its perceived advantages over other electrochemical techniques (Ref 15-19). It enables the system under study to be monitored continuously and without disturbance. It gives information about the kinetics and mechanism of the corrosion process. Moreover, analysis of EN signals generated during metastable pitting state can also provide details about the initiation, propagation, and repassivation processes of this state. EN technique consists of simultaneous measurements of the current and potential noise signals between two or three nominally identical electrodes. The recorded signals can be analyzed by the statistical, the spectral, wavelet, and chaos theory-based methods. EN has received considerable attention in recent years since it was found that the fluctuation of current or potential is closely related to the rate of corrosion reactions or may be used for detection of localized corrosion (Ref 20-25). In the present paper, an attempt was made to study the long-term effect of the exposure of 316SS as well as 316LN SS to the aerated 0.5 M sodium chloride solution vis-à-vis the nucleation or otherwise of the pits, the depth and the growth of the pits and their correlation if any, with the statistical parameters obtained during EN studies, pit initiation sites, etc. Since the welded and fabricated components are stored for a minimum period of 2 years before being put in the service, there is every likelihood of initiation of localized corrosion like pitting or crevice corrosion in the coastal environment of Kalpakkam with high humidity and the presence of chlorides in water due to unforeseen contamination. Therefore, the studies were conducted in aerated 0.5 M NaCl solution to simulate these conditions. Studies conducted using EN technique at open circuit potential (OCP) with the specimens exposed for a long duration to the medium of interest simulate real-life situations. Extensive CLSM studies were conducted on the exposed specimens to study the pit diameters and depths and possible locations of the pitting attack. Apart from exemplifying the superiority of the nitrogen-added stainless steels over the conventional stainless steels, the long-term exposure studies revealed suitability of EN technique over the DC polarization technique in assessing the relative localized corrosion resistance between these steels alongside generating the comprehensive data on the pit depths, diameters, distribution, etc.

2. Experimental

The chemical compositions of the 316SS and 316LN SS used in the present work are given in Table 1. To avoid crevice corrosion attack generally observed in the mounted specimens, corrosion coupons (0.025 m length, 0.018 m breadth and 0.006 m thickness, drilled, and tapped at one end) were used in the present work.

Electrochemical noise studies on this material were performed using two nominally identical coupons of the same size. The coupons were connected to the EN measurement system using threaded specimen rods, which were covered with Teflon tape. The specimens were polished up to 1000 grit finish, washed in soap water and degreased in acetone. Potential and current noise measurements were performed by shorting together two identical working electrodes. The current flowing between the two working electrodes, as well as the potential between the working electrode and a reference electrode were monitored. The area of the specimen exposed to the solution was about 0.0007 m^2.

The potentiostat, which can perform this experiment actively, holds the working electrode connection at the 'ground' potential by a small amplifier circuit. If one 'working' electrode is directly connected to ground and the other is connected to the working electrode cable, they are both held at the same potential and are, in effect, 'shorted' together. Any current, which flows between the two electrodes, is measured by the instruments of current measurement circuits thus creating a Zero Resistance Ammeter (ZRA). The potential is measured between the 'working' electrodes (since they are shorted together, both 'working' electrodes are at the same potential)

Table 1 Chemical composition of the stainless steels, wt.%

Element	316SS	316LN
C	0.050	0.025
Cr	16.92	18.16
Ni	11.67	11.9
Mo	2.19	2.4
N	···	0.067
Mn	1.85	1.62
Si	0.63	0.28
P	0.045	0.044
S	0.015	0.010
Ti	···	0.019
Nb	···	0.032
Cu	···	0.560
Co	···	0.218
B	···	0.0017
W	···	<0.055
Sn	···	<0.004
Pb	···	<0.006
As	···	<0.006
Al	···	0.030
V	···	0.064

and a reference electrode. Saturated calomel electrode (SCE) was used as a reference electrode for the measurement of potential noise.

Electrochemical current and potential noise studies were conducted in aerated 0.5 M sodium chloride solution at OCP and noise signals were collected at the sampling frequency of 1 Hz. The experiment was performed over a period of 30 days to get the information on the long-term exposure of the specimens. Since in EN studies, the signal is mostly non-stationary, the drift or the trend gets introduced. Therefore, the drift or the trend removal was carried out, which is an accepted practice, before calculating the statistical parameters as well as power spectral density (PSD) values. A set of 1024 data points was analyzed to calculate statistical parameters as well as PSD plots. All the potential and current noise data collected in the time domain were transformed after suitably detrending in the frequency domain through the fast Fourier transform (FFT) method, by a dedicated software. To reduce the leakage of the low as well as the high frequencies in the calculated PSD values, Hanning window was used for signal analysis.

2.1 Confocal Microscopy

After the 30 days of exposure, the specimens were washed, dried, and observed under Leica TCS-SP2-RS (Germany) confocal laser scanning microscope (CLSM), equipped with a Leica DMIRE2 inverted microscope and lasers. The images were taken in reflection mode using Ar^{+} ion laser operating at 488 nm and a 40×/0.75 numerical aperture objective lens. All the images were taken by scanning a frame of 512×512 pixels in *x*-*y* plane with the laser beam and each image was averaged over 10 frames for better signal to noise ratio. The 3D images were constructed by stacking the 2D images acquired over several micrometers in *z*-axis.

Morphology of pits, pit diameters and their depths were measured for both steels. The specimens were observed under CLSM at random locations. The information so gathered was analyzed statistically to prepare frequency distribution plots of the pit diameters as well as pit depths.

3. Results and Discussion

Typically, pitting starts in the form of metastable pits which either repassivate before achieving stability or grow to become stable pits. Metastable pits occur over a wide potential range, well below the pitting potential and can be observed electrochemically by the random occurrence of short potential drops or small rise in current transients which vary in magnitude and shape. In the present case, the current and potential time records studied too showed the stage signified by metastable pitting in 316SS stainless steel which were observed 30 min after immersion. The metastable pitting events were marked by sudden but gradual rise and sudden fall of the current signals as shown in Fig. 1(a) for 316SS; concurrently slower drop and the faster rise in the electrode potentials marked the formation of these metastable pits. Similarly, Fig. 1(b) shows the current potential records indicating the occurrence of the metastable pitting in 316LN; however, these events could be observed only after 28 h of immersion. Thus, it was noted that the onset of metastable pitting was much delayed in 316LN compared to 316SS. It has been reported that the passivation properties of the nitrogen-added stainless steels were changed

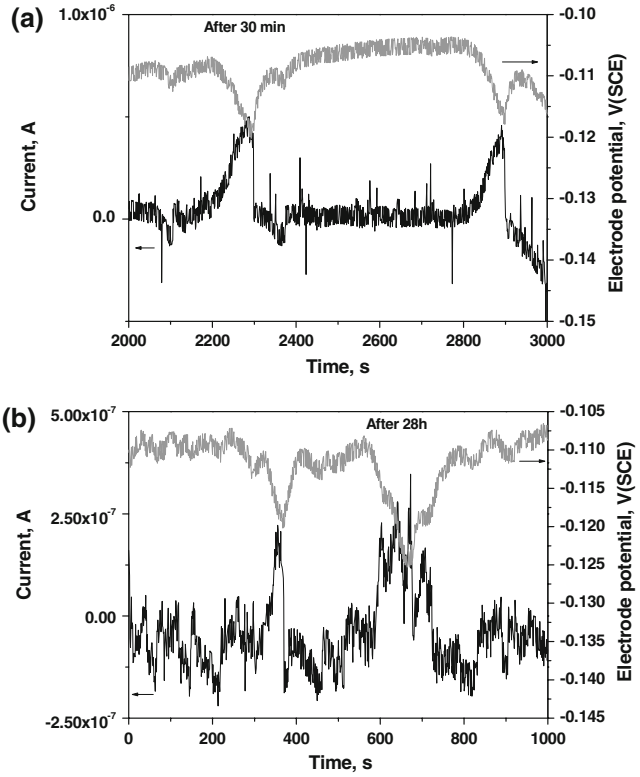

Fig. 1 The metastable pitting events in 316SS (a) and 316LN (b) in aerated 0.5 M NaCl solution at OCP

advantageously leading to an increased pitting potentials and decreased metastable pitting (Ref 26). The drastic reduction in the metastable pitting events in their experiments was ascribed to the addition of 300-400 ppm of nitrogen.

Figure 2a-h shows the current and the potential records at different exposure periods for both the steels; they have been plotted such that out of the total 3600 data points obtained every day for both the steels the corresponding ones at each exposure period were plotted for the sake of comparison. The distinct features exhibited by the current and the potential records of 316SS (Fig. 2a-d) were the faster-onset of the pitting attack and unhindered growth of the stable pits in the aerated sodium chloride solution. Thus, these visual records showed both stable and propagating pits. Each pitting initiation event was indicated by a relatively faster drop in the potential noise, and a much slower rise signifying the repassivation of the pit (Fig. 2c, d). Pistorius (Ref 27, 28), Isaacs (Ref 29), and Pride (Ref 30) found that the rising current transients recorded during pitting corrosion correlated in time with rapid decreases in potential (Fig. 2a, b). Figure 2a typically shows a growing, stable pit. Once a pit starts growing, the current transient increases in a roughly linear fashion, at least for 300-400 s (Ref 31). Once nucleated and stabilized, the growing pits were indicated by distinct broad current peaks that lasted for few hundred seconds with a concurrent drop in the potential (Fig. 2a-d). Figure 2d shows a train of current as well as potential transients for an exposure period of 25 days, which indicated propagation of several pits simultaneously on the surface. It also suggested a total break down of the passivity of the steel at numerous locations on account of the prolonged exposure to the chloride ions. On the other hand, Fig. 2e-h shows that 316LN exhibited the perfect passivity as the

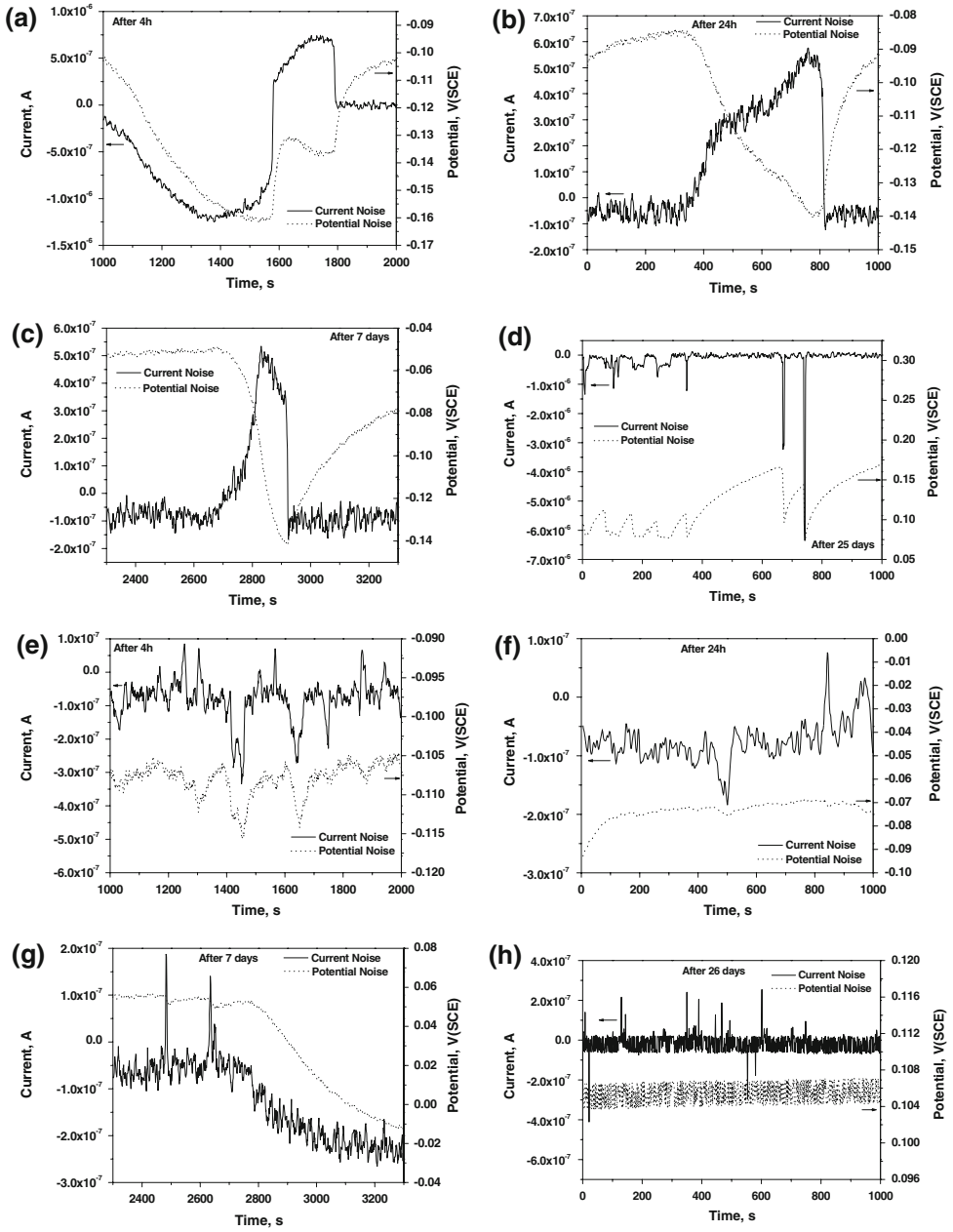

Fig. 2 The current and the potential noise records (1000 s duration) of 316SS (a-d) at 4 h, 24 h, 7 days, 25 days and 316LN SS (e-h) at 4 h, 24 h, 7 days, and 26 days intervals are shown

amplitude of the current transient barely reached 0.2 μA. The current transients observed in these plots could be correlated with the breakdown and repassivation of the passive film at the microscopic sites on the surface like inclusions or secondary phases, etc. Usually, the potential noise pattern for a passive system shows a relatively flat potential time record (Fig. 2f, h). No current transients unlike those observed in 316SS, indicative of stable pitting corrosion were observed even after the prolonged exposure of 26 days. This indicated that 316LN remained completely passive in this medium and the metastable pits that could have formed were promptly repassivated. From the results, it could be gathered that EN technique could be used successfully in distinguishing between the EN patterns of a passive system and that undergoing stable pitting corrosion from the visual records.

The notably used statistical parameters to extract the significant information from the EN data are, standard deviation of current (σ_I), standard deviation of potential (σ_V), and the noise resistance (R_N) which is given by σ_V/σ_I. Earlier it was thought that R_N values were equivalent to R_p, the polarization resistance, but they are not so and are indirectly related to the latter. In fact it is related to spectral noise resistance (R_{SN}) as per the following equations. The R_{SN} is given by Ref 32,

$$R_{SN} = \left[\frac{\Psi_V(f)}{\Psi_I(f)}\right]^{1/2} \quad \text{and} \quad R_N = R_{SN}\,(f \to 0) \qquad \text{(Eq 1)}$$

where, $\Psi_V(f)$ and $\Psi_I(f)$ are the PSD values for the potential and the current, respectively. In fact, R_N values could be more helpful in studying the deterioration of the passive film than

possibly the coefficient of variation of current (CVC) and the pitting index (PI). Although R_N is strictly inversely proportional to the corrosion rate only in the particular case of uniform corrosion under activation control, it is generally accepted that high R_N values are associated to low activity (Ref 33). Thus, R_N values could be used to indicate the high- or low-corrosion activity. Presently, R_N as well as R_{SN} ($f \rightarrow 0$) values were plotted (Fig. 3a, b) for both the steels. It was observed that R_N values for 316SS (Fig. 3a) gradually deteriorated with exposure time; a linear fit showed (R_N = 28571.78 – 805 * time (d)). The R^o_{SN} plot for 316SS showed some scatter, but largely followed the decreasing trend with time. On the other hand, R_N values for 316LN (Fig. 3b) after going through the initial hump steadied and remained almost constant with time of exposure. The same trend was observed with the R^o_{SN} plot too. In case of 316SS the R_N value deteriorated from the initial value of 34746-7138 Ω cm^{-2} on the 30th day whereas in case of 316LN the initial R_N value of 28815 Ω cm^{-2} changed to 23306 Ω cm^{-2} on the 30th day. Therefore, it was noted that there was a rapid deterioration in the R_N values in 316SS whereas the R_N values in 316LN were fairly stable. Thus, it was obvious that the deterioration of R_N values in 316SS could have resulted from the insidious pitting attack which increased with exposure time and the invariant trend in R_N values for 316LN could have resulted from either the lack of pitting corrosion or rapid repassivation of the initiated pits.

Figures 4(a, b) and 5(a, b) show the plots of the mean current and mean potential of the noise data as well as the current noise (in dB) at ($f \rightarrow 0$), respectively, for both the steels. A noisy mean current and the mean potential plot (Fig. 4a) of 316SS along with the increasing current (dB) plot (Fig. 5a) clearly indicated the pitting corrosion activity that resulted in the steady rise in the current (dB) values. Earlier it was reported that the power level of the signal as calculated from the PSD in the frequency-independent region seemed to indicate the corrosion rate (Ref 34) which supported the increased pitting corrosion activity observed in 316SS as shown in Fig. 5(a). As against this, the plots of mean current and the mean potential (Fig. 4b) for 316LN showed a trend, which was invariant with time with some scatter in the early part of the exposure. The current (dB) plot (Fig. 5b) for 316LN showed a clear downward trend indicating a continuous repassivation of the unstable pits and the build up of the passive film. This observation is in perfect line with the earlier observation that the nitrogen in the solid solution of the stainless steel facilitated the repassivation (Ref 14). It has been observed in some of the crevice corrosion tests using the nitrogen-added stainless steels that the surface of the crevice was covered with the chromium oxides, iron oxides, and nitrogen in the form of nitrides and NH_3 (Ref 35).

In general, the characteristic charge (Q) and frequency (F) associated with the events constituting the corrosion process can be related to the amount of metal lost in each of the events

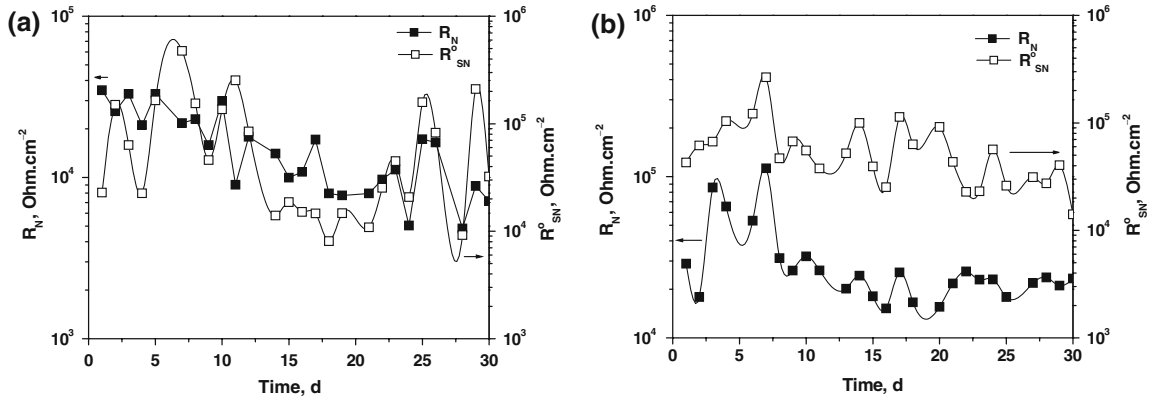

Fig. 3 R_N and R^o_{SN} plots for 316SS (a) and 316LN (b) in aerated 0.5 M sodium chloride solution

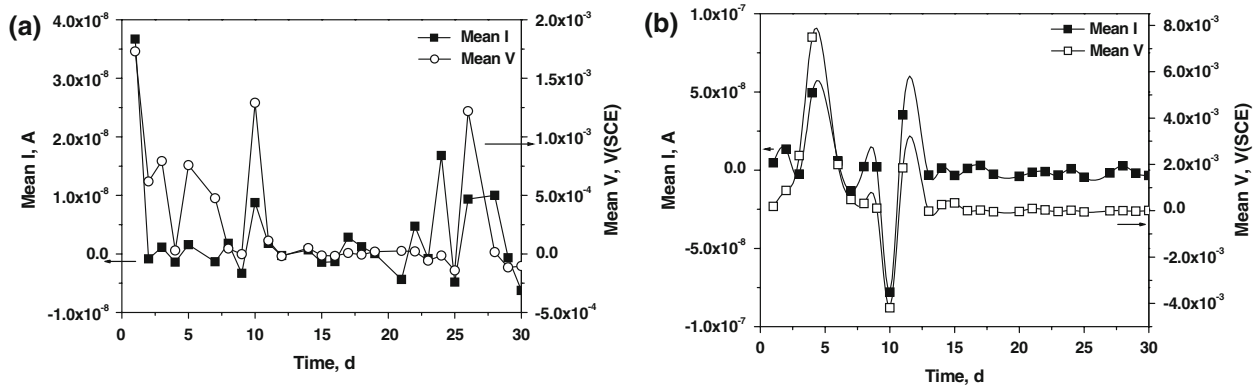

Fig. 4 The plots of Mean I and Mean V for 316SS (a) and 316LN (b) in aerated 0.5 M sodium chloride solution

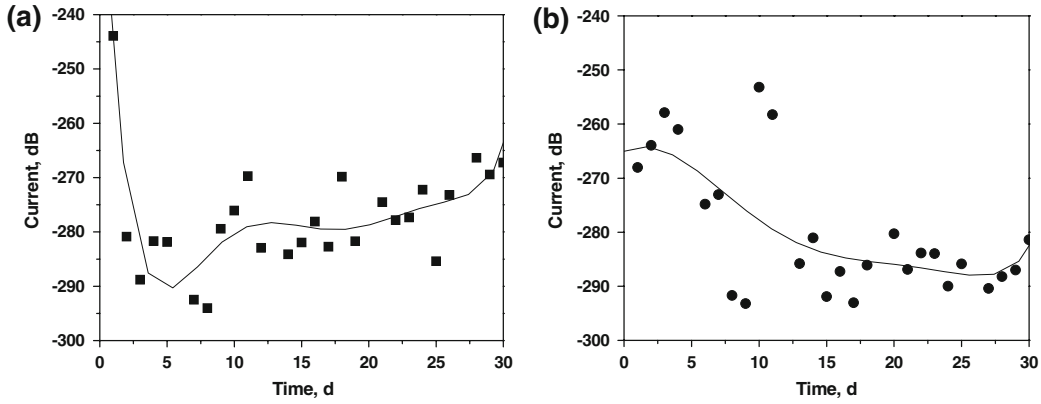

Fig. 5 The plots of current, dB ($f \rightarrow 0$) values for 316SS (a) and 316LN (b) in aerated 0.5 M sodium chloride solution

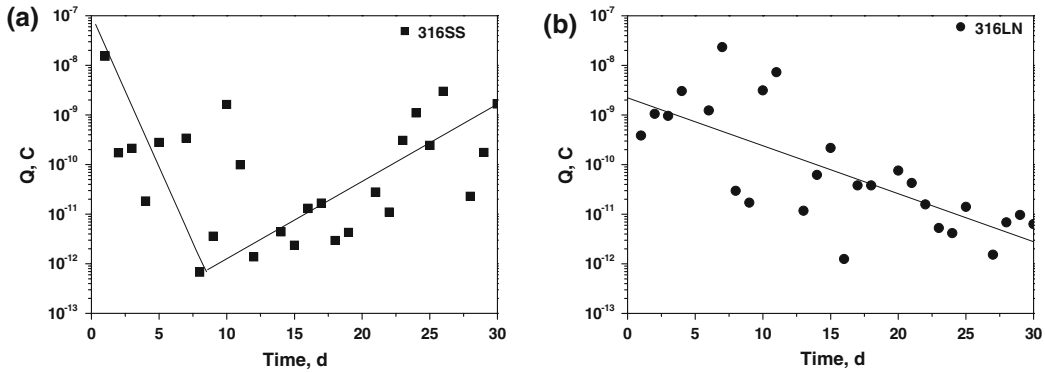

Fig. 6 The characteristic charge (Q) plots for 316SS (a) and 316LN (b) in aerated 0.5 M sodium chloride solution

and the rate at which these events occur, respectively. According to Cottis et al. (Ref 15, 36-37), these parameters were estimated based on shot noise analysis at very low frequency limit of the $PSD_{i,v}$ plots (white region) and expressed by the following equations:

$$Q = (PSD_i \times PSD_v)^{0.5}/B \qquad \text{(Eq 2)}$$

where B is the Tafel coefficient. In these calculations, the B value was taken to be 0.026 V per decade (Ref 15). This result is obtained for common values of the Tafel slopes for the anodic and cathodic reactions. From the plots of the characteristic charge against time of exposure for the steels (Fig. 6a, b), it was observed that, in spite of the scatter in the data points, two best fit intersecting lines could be obtained for 316SS; from these lines, it could be observed that initially the Q value continuously decreased linearly and thereafter there was a linear rise in Q. The increase in the value of Q is attributed to an increase in the localized corrosion which is associated with large transients and consequently large values of charge (Ref 36). Thus, the linear rise in Q was attributed to the increase in the formation of stable pits in 316SS and their unabated growth. However, there was a continuous and a linearly decreasing trend in Q in case of 316LN which was attributed to the repassivation of the metastable pits and strengthening of the passive film.

Most of the pits in 316SS that were observed under CLSM were found to be circular (but not exclusively, as some of the pits with irregular shapes too were observed) at the opening and were found to have attacked the alloy in a vertical fashion, thus helping to measure the pit depths. Two large pits, somewhat spherical one initiated due to the polishing line as well as the one with an irregular shape have been shown in Fig. 7(a, b). The other smaller pits growing in the vicinity of the irregularly shaped pit shown in Fig. 7(b) are clearly visible. The statistical information about the observation of pits observed under CLSM was categorized under frequency plots for the pit diameters as well as the pit depths (Fig. 8a, b). The frequency distributions of pit diameters as well pit depths were observed to be highest at 10-20 and 5-10 μm, respectively. However, pits with as large as 70-80 μm diameters and as deep as 20-25 μm too were observed. The pitting corrosion attack of this nature in the stationary aerated 0.5 M sodium chloride solution could be considered to be quite serious in nature. Figure 9(a, b) shows the 2D and the 3D photomicrographs of a large pit grown on 316SS after the 30 days of exposure. The 2D photomicrograph showed a centrally located and somewhat shiny object, which could be possibly, an inclusion. The 3D photomicrograph showed that the pits could have got initiated at the opposite ends of the same inclusion and grown independently; this picture gives the fair idea about the depth of the pit, which is about 10 μm. Figure 10(a, b) shows the 2D and the 3D photomicrographs of a shallow pit in 316LN after 30 days of exposure. The 2D photomicrograph showed the bright shiny metal, which was nothing but the passivated steel at the shallow pit bottom. The 3D photomicrograph showed the shallowness of the pitting attack along with the polishing lines that were visible even through the pit interior, indicating a shallow pit, which got

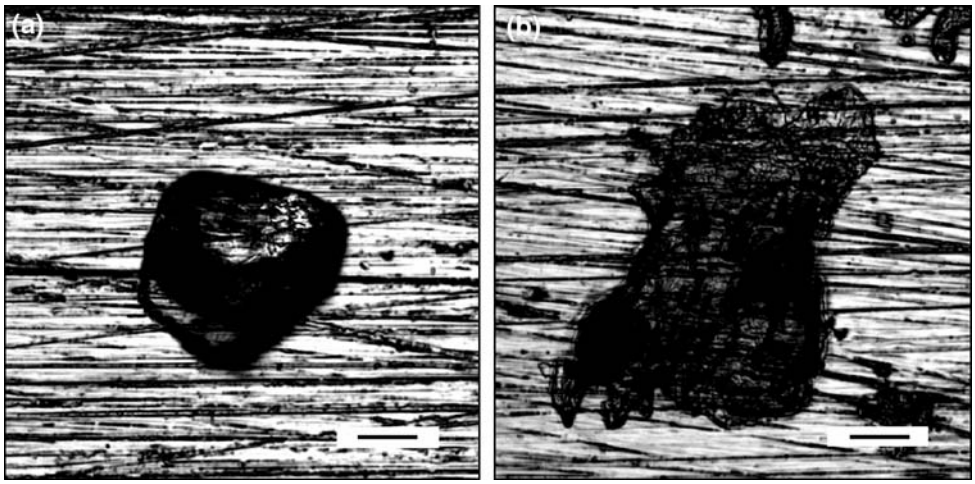

Fig. 7 The morphology of the pits observed in 316SS (a, b) at the end of 30 days exposure in aerated 0.5 M sodium chloride solution. The marker on the photomicrograph is equal to 20 μm

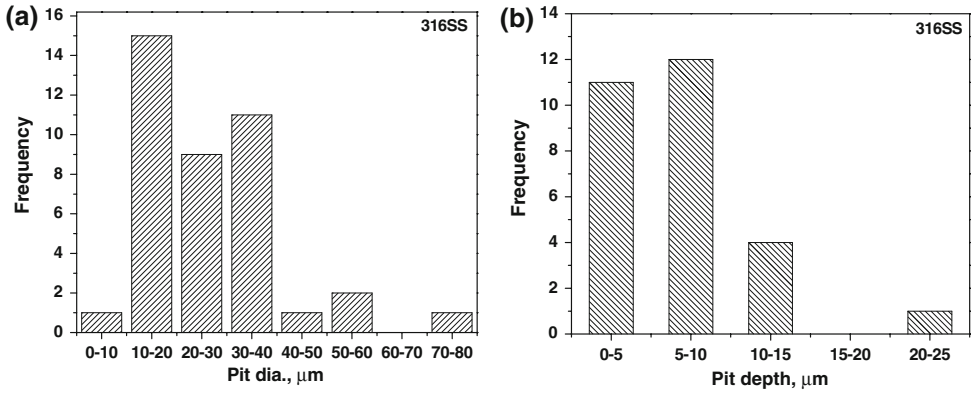

Fig. 8 The histograms showing the frequency distribution for the pit diameters and the pit depths for 316SS in aerated 0.5 M sodium chloride solution

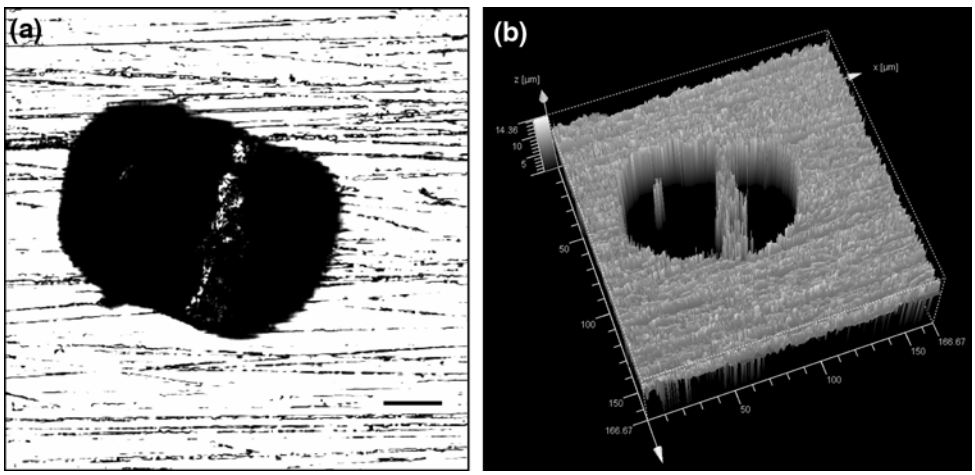

Fig. 9 The 2D (a) and the 3D (b) photomicrograph of a deep (same) pit on 316SS taken using CLSM showing a large pit with its undissolved portion in the 3D photomicrograph. The horizontal bar in 2D picture is equal to 20 μm

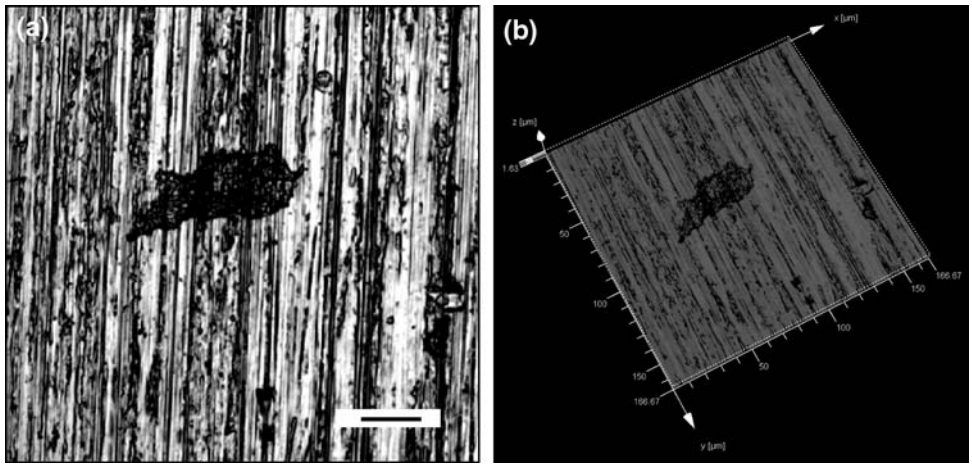

Fig. 10 The 2D (a) and the 3D (b) photomicrograph of a shallow (same) pit on 316LN taken using CLSM showing a pit with its shallow base in the 3D photomicrograph. The horizontal bar in 2D picture is equal to 20 µm

repassivated and stopped growing. The depth measurement of some of the pits observed in 316LN steel could not be accomplished satisfactorily owing to the fact that, the depths of these pits were <300 nm, thereby indicating that these were the pits that were repassivated immediately. These observations concur well with the recent information that Mo and N promoted the passivation by formation of more stable passive film and the repassivation by increasing the formation rate of passive film, and that the exact mechanisms of the role of Mo and N on the repassivation kinetics and the exact interaction between N and Mo remained still to be clarified (Ref 38).

4. Conclusions

From the investigations conducted on the long-term exposure of 316SS and 316LN to the aerated 0.5 M sodium chloride solution, the following conclusions could be drawn:

(1) Comprehensive localized corrosion data could be obtained using EN technique at OCP which otherwise could not have been obtained using the conventional DC polarization technique. The system under study also presents the real-life situation for the stainless steel components fabricated, stored, and subjected to localized corrosion at OCP in the humid coastal environment.
(2) From the visual records as well as the analysis of the statistical parameters, it could be noted that EN technique could be usefully utilized in distinguishing between a perfectly passive system and the one undergoing pitting corrosion.
(3) The inferior localized corrosion resistance of 316SS is owing to the lack of the repassivating ability of its passive film and the presence of inclusions and other homogeneities that allow the initiation of the pits, which grow unhindered in aerated 0.5 M NaCl solution. The repassivated pits on 316LN SS showed its excellent localized corrosion resistance after 30 days of exposure.
(4) The excellent resolution of CLSM technique helps to study the 2D and 3D morphology of the pit diameters as well as depths, which can help in judging the gravity of the localized corrosion attack. This technique can be further used to characterize completely the single pit generated on SS surface under controlled experimental conditions and to study the pit growth kinetics.

References

1. M.G. Fontana, Ed., *Corrosion Engineering*. McGraw-Hill, New York, 1987, p 71
2. G. Wranglen, Pitting and Sulphide Inclusions in Steel, *Corros. Sci.*, 1974, **14**(5), p 331–349
3. G.S. Eklund, Initiation of Pitting at Sulfide Inclusions in Stainless Steel, *J. Electrochem. Soc.*, 1974, **121**(4), p 467–473
4. D.W. Williams and Y.Y. Zhu, Explanation for Initiation of Pitting Corrosion of Stainless Steels at Sulfide Inclusions, *J. Electrochem. Soc.*, 2000, **147**(5), p 1763–1766
5. J. Stewart and D.E. Williams, The Initiation of Pitting Corrosion on Austenitic Stainless Steel: On the Role and Importance of Sulphide Inclusions, *Corros. Sci.*, 1992, **33**(3), p 457–463
6. J.E. Castle and R. Ke, Studies by Auger Spectroscopy of Pit Initiation at the Site of Inclusions in Stainless Steel, *Corros. Sci.*, 1990, **30**(4–5), p 409–428
7. M.A. Baker and J.E. Castle, The Initiation of Pitting Corrosion at MnS Inclusions, *Corros. Sci.*, 1993, **34**(4), p 667–682
8. L.L. Shreir, R.A. Jarman, G.T. Burstein, Eds., *Corrosion, Vol. 1, Metal/Environment Reactions*. 3rd ed., Butterworth-Heinemann, Oxford, 1994, p 3:47
9. G.C. Palit, V. Kain, and H.S. Gadiyar, Electrochemical Investigations of Pitting Corrosion in Nitrogen-Added Type 316LN Stainless Steel, *Corrosion*, 1993, **49**(12), p 977–991
10. R.F.A. Jargelius-Pettersson, Electrochemical Investigation of the Influence of Nitrogen Alloying on Pitting Corrosion of Austenitic Stainless Steels, *Corros. Sci.*, 1999, **41**(8), p 1639–1664
11. S.D. Chyou and H.C. Shih, The Effect of Nitrogen on the Corrosion of Plasma-Nitrided 4140 Steel, *Corrosion*, 1991, **47**(1), p 31–34
12. H.J. Grabke, The Role of Nitrogen in the Corrosion of Iron and Steels, *ISIJ Intl.*, 1996, **36**(7), p 777–786
13. I. Olefjord and L. Wegrelius, The Influence of Nitrogen on the Passivation of Stainless Steels, *Corros. Sci.*, 1996, **38**(7), p 1203–1220
14. H. Baba, T. Kodama, and Y. Katada, Role of Nitrogen on the Corrosion Behavior of Austenitic Stainless Steels, *Corros. Sci.*, 2002, **44**(10), p 2393–2407
15. R.A. Cottis, Interpretation of Electrochemical Noise Data, *Corrosion*, 2001, **5**(3), p 265–285
16. D.A. Eden, Electrochemical Noise—The First Two Octaves, *CORROSION/98*, Paper no. 386, National Association of Corrosion Engineers, Houston, TX, 1998

17. J. Smulko and K. Darowicki, Nonlinearity of Electrochemical Noise Caused by Pitting Corrosion, *J. Electroanal. Chem.*, 2003, **545**, p 59–63
18. A. Aballe, M. Bethencourt, F.J. Bonata, and M. Marcos, Using Wavelet Transform in the Analysis of Electrochemical Noise Data, *Electrochim. Acta*, 1999, **44**, p 4805–4816
19. U. Bertocci, C. Gabrielli, F. Huet, and M. Keddam, Noise Resistance Applied to Corrosion Measurements: 1. Theoretical Analysis, *J. Electrochem. Soc.*, 1997, **144**(1), p 31–37
20. R.G. Hardon, P. Lambert, and C.L. Page, Relationship Between Electrochemical Noise and Corrosion Rate of Steel in Salt Contaminated Concrete, *Br. Corros. J.*, 1988, **23**(4), p 225–228
21. F. Carassiti, R. Cigna, G. Gusmano, and R. Goolamallee, Detection of Localized Corrosion by Means of Statistic and Harmonic Analysis of Spontaneous Potential Noise, *Mater. Sci. Forum*, 1989, **44/45**, p 271–278
22. J.C. Uruchurtu and J.L. Dawson, Noise Analysis of Pure Aluminum Under Different Pitting Conditions, *Corrosion*, 1987, **43**(1), p 19–26
23. Y.-J. Tan, N.N. Aung, and T. Liu, Novel Corrosion Experiments Using the Wire Beam Electrode. (I) Studying Electrochemical Noise Signatures from Localised Corrosion Processes, *Corros. Sci.*, 2006, **48**(1), p 23–38
24. I.A. Al-Zanki, J.S. Gill, and J.L. Dawson, Electrochemical Noise Measurements on Mild Steel in 0.5 M Sulphuric Acid, *Mater. Sci. Forum*, 1986, **8**, p 463
25. P.C. Searson and J.L. Dawson, Analysis of Electrochemical Noise Generated by Corroding Electrodes Under Open-Circuit Conditions, *J. Electrochem. Soc.*, 1988, **135**(8), p 1908–1915
26. Y.S. Lim, J.S. Kim, S.J. Ahn, H.S. Kwon, and Y. Katada, The Influences of Microstructure and Nitrogen Alloying on Pitting Corrosion of Type 316L and 20 wt.% Mn-Substituted type 316L Stainless Steels, *Corros. Sci.*, 2001, **43**, p 53–68
27. P.C. Pistorius, The Effect of Some Fundamental Aspects of the Pitting Corrosion of Stainless Steel on Electrochemical Noise Measurements, *Electrochemical Noise Measurement for Corrosion Applications*, J.R. Kearns, J.R. Scully, P.R. Roberge, D.L. Reichert, and J.L. Dawson, Eds., ASTM STP 1277, West Conshohocken, 1996, p 343
28. P.C. Pistorius, Design Aspects of Electrochemical Noise Measurements for Uncoated Metals: Electrode Size and Sampling Rate, *Corrosion*, 1997, **53**(4), p 273–283
29. H.S. Isaacs and Y. Ishikawa, Current and Potential Transients During Localized Corrosion of Stainless Steel, *J. Electrochem. Soc.*, 1985, **132**(6), p 1288–1293
30. S.T. Pride, J.R. Scully, and J.L. Hudson, Analysis of Electrochemical Noise from Metastable Pitting in Aluminum, Aged Al-2% Cu, and AA 2024–T3, *Electrochemical Noise Measurement for Corrosion Applications*, J.R. Kearns, J.R. Scully, P.R. Roberge, D.L. Reichert, and J.L. Dawson, Eds., ASTM STP 1277, West Conshohocken, 1996, p 307
31. U. Bertocci and Y. Yang-Xiang, An Examination of Current Fluctuations During Pit Initiation in Fe-Cr Alloys, *J. Electrochem. Soc.*, 1984, **131**(5), p 1011–1017
32. X.Y. Zhou, S.N. Lvov, X.J. Wei, L.G. Benning, and D.D. Macdonald, Quantitative Evaluation of General Corrosion of Type 304 Stainless Steel in Subcritical and Supercritical Aqueous Solutions Via Electrochemical Noise Analysis, *Corros. Sci.*, 2002, **44**(4), p 841–860
33. J.M. Sanchez-Amaya, R.A. Cottis, and F.J. Botana, Shot Noise and Statistical Parameters for the Estimation of Corrosion Mechanisms, *Corros. Sci.*, 2005, **47**(12), p 3280–3299
34. A. Al-Zanki, J.S. Gill, and J.L. Dawson, Electrochemical Noise Measurements on Mild Steel in 0.5 M Sulphuric Acid, *Mater. Sci. Forum*, 1986, **8**, p 463–476
35. H. Baba and Y. Katada, Effect of Nitrogen on Crevice Corrosion in Austenitic Stainless Steel, *Corros. Sci.*, 2006, **48**(9), p 2510–2524
36. R.A. Cottis, M.A.A. Al-Awadhi, H. Al-Mazeedi, and S. Turgoose, Measures for the Detection of Localized Corrosion with Electrochemical Noise, *Electrochim. Acta*, 2001, **46**(24–25), p 3665–3674
37. H.A. Al-Mazeedi, R.A. Cottis, and S. Turgoose, Electrochemical Noise Analysis of Carbon Steel in Sodium Chloride Solution with Sodium Nitrite as an Inhibitor, *Proceedings of Eurocorr 2000*, Institute of Materials, London, 2000
38. Jae-Bong Lee, Effects of Alloying Elements, Cr, Mo and N on Repassivation Characteristics of Stainless Steels Using the Abrading Electrode Technique, *Mater. Chem. Phys.*, 2006, **99**(2–3), p 224–234